RESEARCH PAPER

Environmentally and Ecofriendly of Photocatalytic Activity of CdS/ZnO Nanocomposite Synthesized via Hydrothermal Method for Methylene Blue Degradation by Using UVA Light

Tameem Albassam [1], Asia Ali Hamza [2], Sarmad Jaafar Mohammed Alrubaye [3], Hayder Hamid Abbas Al-Anbari [4], Shaima Abd [5], Zuhair I. Al-Mashhadani [6], Wael Dheaa Kadhim [7]*

[1] *Department of Dentistry, Dijlah University College, Baghdad, Iraq*
[2] *Department of Clinical Laboratory Sciences, University of Alkafeel, Iraq*
[3] *College of Medicine, University of Al-Ameed, Kerbala, Iraq*
[4] *Ahl Al bayt University, College of Pharmacy, Kerbala, Iraq*
[5] *Department of Sciecnes, Al-Manara College for Medical Sciences, Maysan, Iraq*
[6] *Department of Medical Laboratories Technology, AL-Nisour University College Baghdad, Iraq*
[7] *Mazaya University College, Iraq*

ARTICLE INFO

Article History:
Received 10 January 2025
Accepted 25 March 2025
Published 01 April 2025

Keywords:
CdS/ZnO nanocomposite
Decolonization
Methylene blue dye
Photocatalytic

ABSTRACT

This study investigates the photocatalytic efficiency of a CdS/ZnO nanocomposite for the decolorization of the cationic dye Methylene Blue (MB). The physicochemical characteristics of the synthesized nanocomposite were systematically characterized using X-ray Diffraction (XRD), Field Emission Scanning Electron Microscopy (FESEM), Energy Dispersive X-ray Spectroscopy (EDX), and Transmission Electron Microscopy (TEM). The photocatalytic performance of the CdS/ZnO nanocomposite, functioning as a semiconductor catalyst, was evaluated for the degradation of MB in aqueous solution under UV light irradiation within a slurry photo-reactor system. A comprehensive assessment of operational parameters, including catalyst dosage and initial dye concentration, was conducted to determine their influence on the decolorization kinetics. The results revealed that the photocatalytic decolorization of MB followed a two-stage kinetic process, exhibiting an initial rapid decolorization phase followed by a slower reaction phase. Enhanced decolorization efficiency was observed with decreasing initial MB concentration and increasing UV light intensity. The optimal catalyst loading was identified as approximately 20 $mg \cdot L^{-1}$, while the most favorable pH for the reaction was around 6.8, aligning with the natural pH of the MB solution.

How to cite this article
Albassam T., Hamza A., Alrubaye S., Al-Anbari H. et al. Environmentally and Ecofriendly of Photocatalytic Activity of CdS/ZnO Nanocomposite Synthesized via Hydrothermal Method for Methylene Blue Degradation by Using UVA Light. J Nanostruct, 2025; 15(2):525-533. DOI: 10.22052/JNS.2025.02.013

INTRODUCTION

It has recently come to light that industrial wastewater is the primary source of azo dyes. The dye's structure is mainly stable. Many dangerous compounds were present as a result of the dye's incomplete breakdown. Therefore, it is essential to remove harmful colors from natural water sources. Since many manufacturing companies

* *Corresponding Author Email: mashhadani.zuhair@gmail.com*

release synthetic dyes in large quantities, they make up a significant portion of industrial water effluents [1-3]. Due to the compounds' propensity to cause cancer, the effects of these dyes on the environment are a serious worry. Additionally, the anaerobic decolonization of certain dyes can lead to the formation of carcinogens. Both sunlight penetration and oxygen dissolution, which are vital for aquatic life, can be blocked by wastewater that has been colored with these dyes. Therefore, it is imperative that these colored effluents be treated before being released into different bodies of water. The literature has reported various methods for treating and decontaminating such effluents. Classical procedures, including adsorption, coagulation, ion flotation, and sedimentation, are examples of typical approaches [4-7].

Although all these methods are practical and adaptable, they all generate a secondary waste product that requires further processing. Advanced Oxidation Processes (AOPs), a relatively recent, more potent, and promising set of procedures, have been developed and utilized to treat wastewater effluents contaminated with dyes.Typically, this process uses a potent oxidizing species, such as OH radicals, which are generated in situ and initiate a series of events that reduce the macromolecules to smaller, less hazardous forms. The macromolecule is frequently fully mineralized into carbon dioxide and water. The AOP technique has garnered considerable interest from the scientific community due to its simplicity and lower yield requirements [8-13].

Several physicochemical methods are available for removing dyes from wastewater. However, photocatalysis is a more promising approach. Additionally, photocatalysis can break down a dye molecule and induce redox changes. Due to their environmentally friendly advantages in conserving resources such as water, energy, chemicals, and other cleaning supplies, photosensitive semiconductors like TiO_2, ZnO, Fe_2O_3, CdS, ZnS, and V_2O_5 have been utilized in the literature to reduce the color of dye solutions.

The majority of synthetic colorants (60–70%) are azo dyes, which are used in the manufacturing of textiles, paper, leather, gasoline, additives, foodstuffs, cosmetics, laser materials, xerography, laser printing, and other products. The byproducts that are produced from these processes contain both dyes and metal ions. Since only 45–47% of dyestuffs have been shown to be biodegradable, insoluble dyes with poor biodegradability are primarily responsible for any remaining color [14, 15]. Nitrogen-to-nitrogen double bonds (–N=N–) that are often bonded to two moieties, at least one of which is typically an aromatic group (such as benzene or naphthalene rings), define

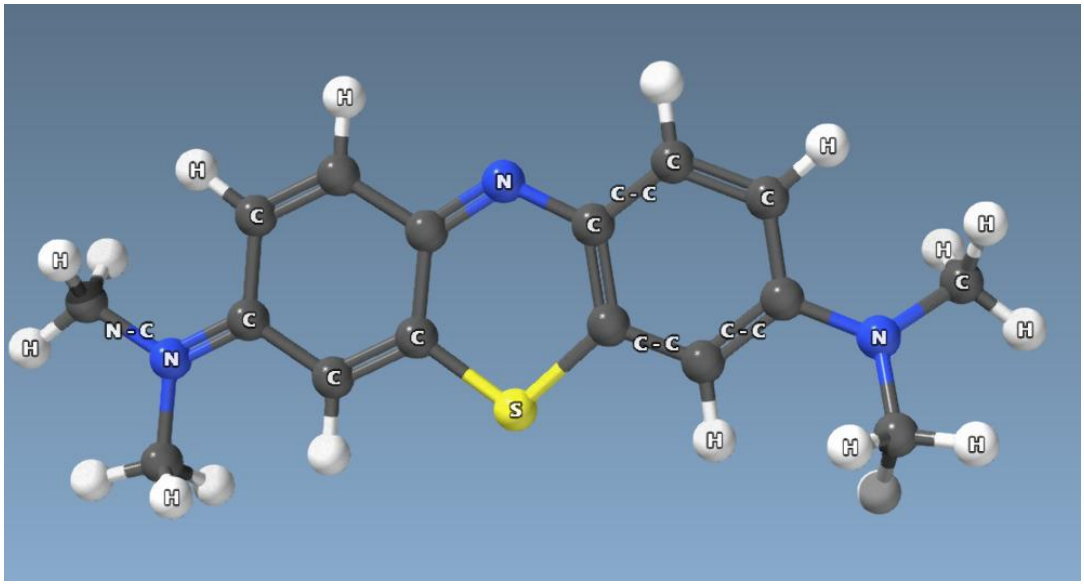

Fig. 1. Chemical structure of MB dye in 3D view.

azo dyes. Methyl Orange, Acid Orange 20, Direct Blue 160, Disperse Orange 1, Basic Blue 41, Amido Black, Amaranth, and so on are a few exemplary examples of azo dyes. The azo dyes can be categorized as monoazo (Acid orange 7, Orange G, Methyl red, etc.), diazo (Congo Red), or triazo (Reactive red 120, Naphthol blue black, etc.) based on the number of -N=N-groups in the molecule [16-19].

MATERIALS AND METHODS

Chemicals

The following chemical reagents were utilized (Sigma-Aldrich): MB (99% the chemical structure shown in Fig. 1), methanol (CH_3OH, 995%), hydrogen peroxide (H_2O_2, 23%), ethanol (CH_3CH_2OH, 98.5%), sodium sulfide (Na_2S, 95%), reducing agents, cadmium acetate dehydrate ($Cd(CH_3COO)_2{\cdot}2H_2O$, 99.5%), and zinc oxide (ZnO NPs, 99.5%).

Synthesis of CdS /ZnO nanocomposite

Initially, 10 mL of 1g sodium sulfide (Na_2S) was added drop-by-drop into a 20 mL solution of 2 g cadmium acetate dehydrate ($Cd(CH_3COO)_2{\cdot}2H_2O$) that had been combined with 2 g zinc oxide (ZnO NPs). Before being placed in a hydrothermal system and heated to 160 °C for 24 hours in an autoclave, the mixture was magnetically agitated for 1 hour at 25 °C. The mixture was then repeatedly cleaned with distilled water and dried for 24 hours at 60 °C in an oven, the suggested strcutre shown in Fig. 2.

Photodegradation procedure

A solution with a known dye concentration was made for the photo-degradation of MB dye. It was then left to equilibrate in the dark for 15 minutes. After that, 200 milliliters of the suspension were moved to a 300-ml beaker. After making the necessary adjustments, the dye's pH value was 6.8. The reaction was then started by turning on the lamp. The suspension was kept homogeneous during irradiation by maintaining agitation, and it was sampled following the proper illumination duration. Using a calibration curve and a UV-Vis spectrophotometer set to λmax = 663 nm, the amount of dye in each deteriorated sample was measured. The conversion percentage of MB dye can be obtained at various intervals using this procedure. The following provides the photo-degradation efficiency (DE%):

$$DE\ \% = ((C_f - C_i)/C_f) \times 100 \quad (1)$$

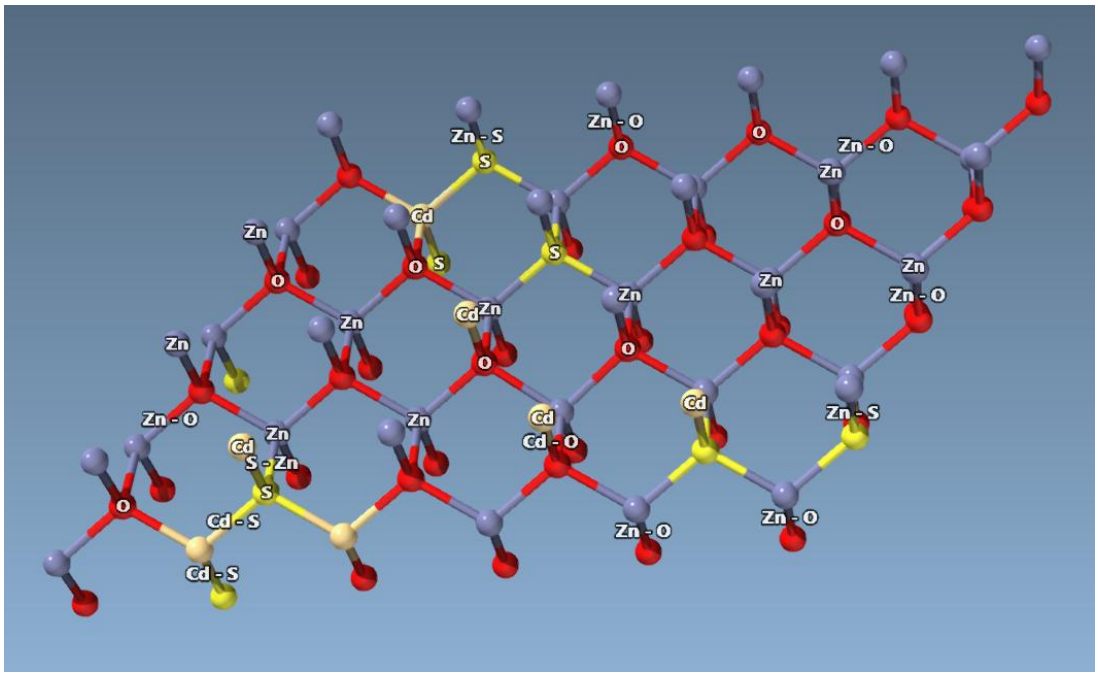

Fig. 2. 3D structure of CdS/ZnO nanocomposite cluster.

RESULTS AND DISCUSSION

Surface Characterizations

The SEM images of the ZnO sample are displayed in Fig. 3. The spherical 3D structure, approximately 500 nm in size, is depicted in Fig. 3a. The CdS/ZnO particles exhibit a morphology of nanosheets that are interconnected to form a three-dimensional structure, as shown in Fig. 3b, which was acquired at a magnification of 500 nm.

It was discovered that the TEM picture limited the ability to determine the crystal structure, particle size, and shape. And, as seen in Fig. 3, the average size of ZnO-CdS NPs at 100 nm. ZnO-CdS crystal structure and surface morphology were described. The ZnO-CdS surface is seen in Fig. 3c as a white, spherical structure. Furthermore, a black spherical structure formed as a result of loading CdS onto the surface of zinc oxide nanoparticles after the loading procedure. This successful loading reassures us of the effectiveness of our process. The EDX of the CdS/ZnO confirms the presence of Zn, Cd, and O, as shown in Fig. 3d [20-22].

X-ray diffraction (XRD) analysis to estimate the crystalline phase and purity of the prepared ZnO-CdS NPs. The results showed that the samples possess a high degree of crystallinity and purity, as evidenced by the sharp peaks in their appearance. XRD pattern of ZnO- CdS NPs (Fig. 4) showed reflections at 2θ values of (18.81 °, 22.02°, 24.41 °,28.94 °, 32.06 ° 35.06 ° , 38.06 ° and 55.51 °) for ZnO-CdS nanocomposite, which correspond to reflections from crystal planes. (111), (100), (002), (101), (102,220), (110,311), (103), and (112), respectively. Clearly and distinctly, the position of the ZnO peaks was slightly shifted towards higher 2θ values compared to pure ZnO [23, 24].

Effect of the weight of Cd/ZnO nanoparticles

The effect of photocatalyst concentration (ranging from 0.1 to 0.4 g) on the photodegradation

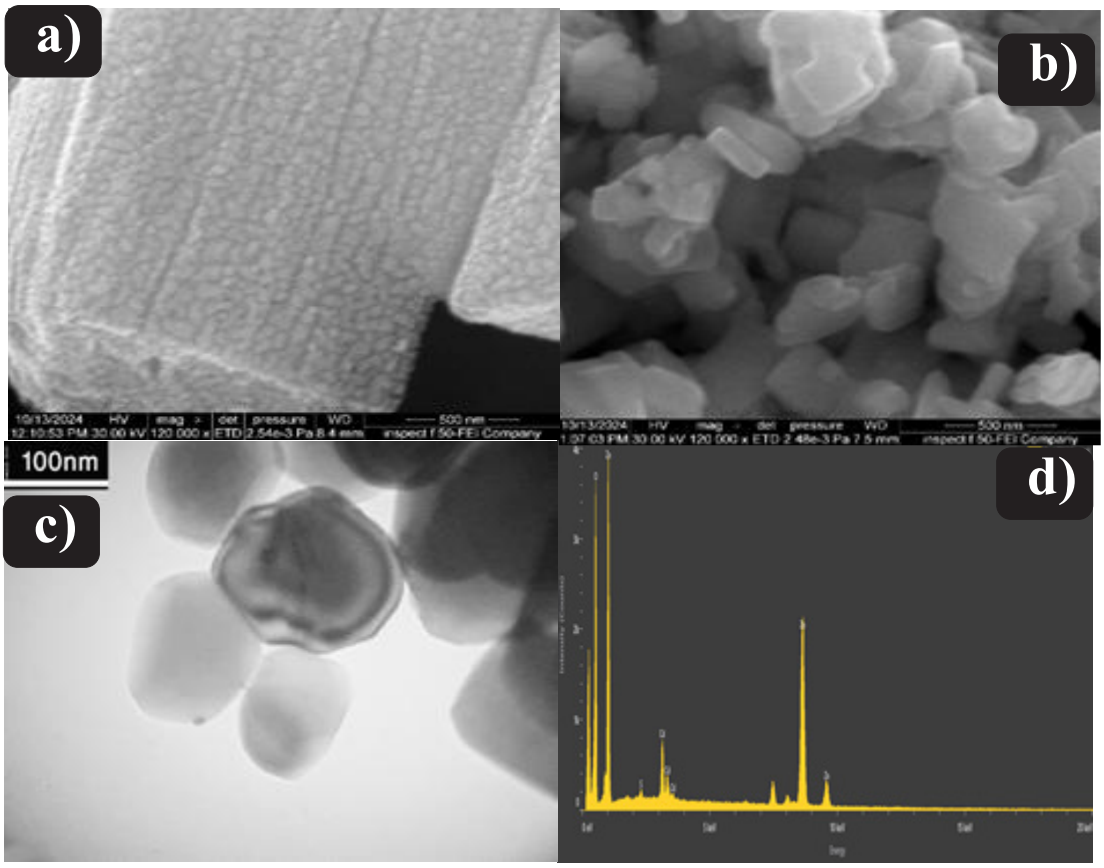

Fig. 3. FESEM image a) ZnO, b) ZnO /CdS, c) TEM of ZnO/CdS, and d) EDX of ZnO/CdS.

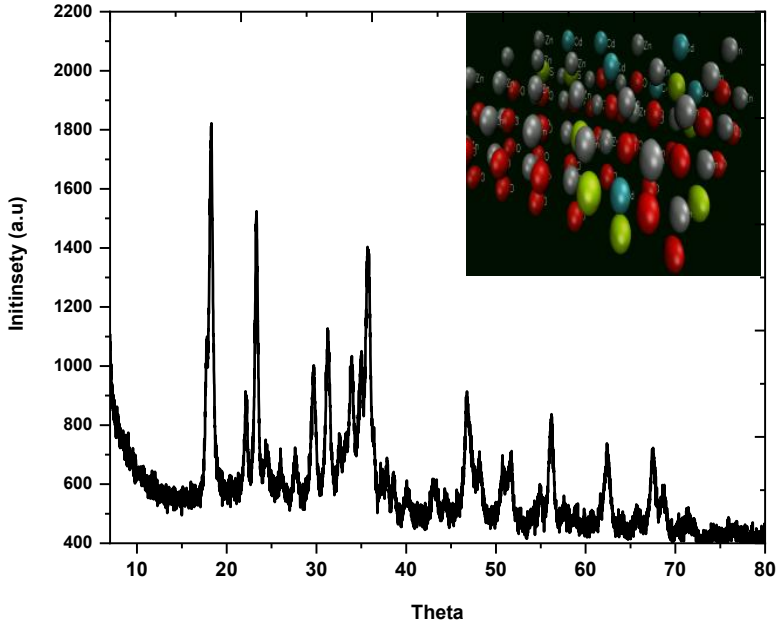

Fig. 4. XRD of ZnO-CdS structure.

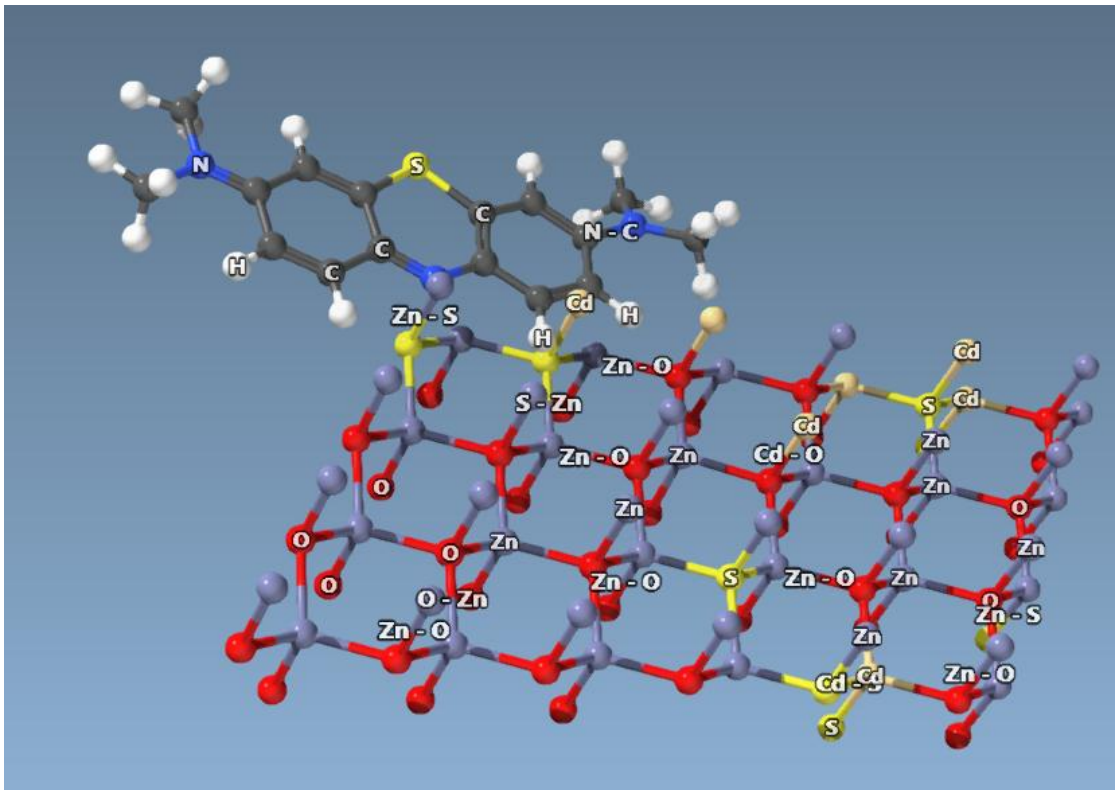

Fig. 5. Suggested interaction for adsorption process between MB and ZnO/CdS nanocomposite.

of MB dye was investigated at a dye concentration of 20 mg/L, a light intensity of 2.1 mW/cm², an O_2 flow rate of 5 mL/min, and a pH of 7.1. At concentrations below 0.2 g/L, increasing the photocatalyst concentration resulted in a higher rate of dye photodegradation, the photodegradation

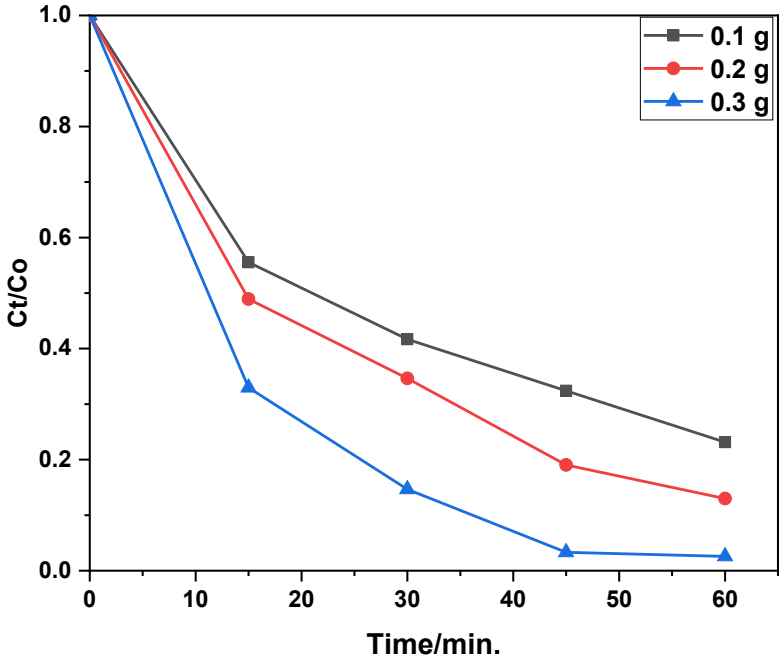

Fig. 6. Effect of the weight of Cd/ZnO nanoparticles on photocatalytic degradation MB dye.

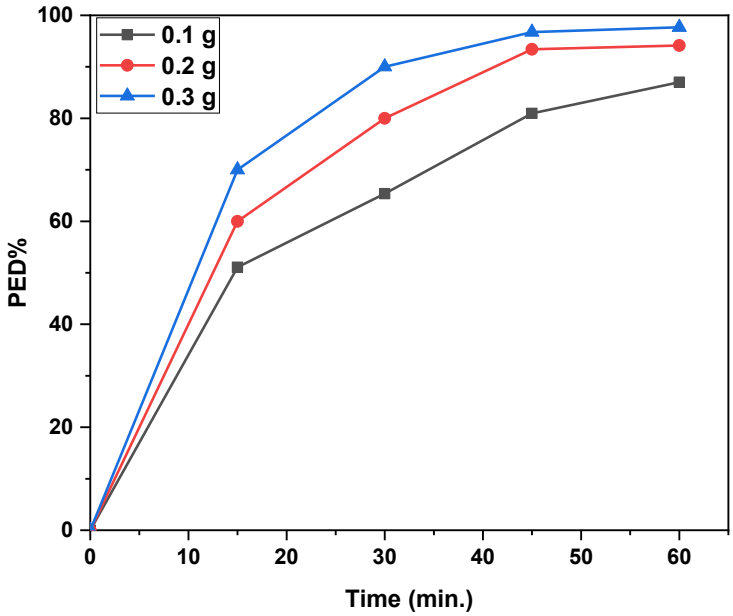

Fig. 7. Effect of mass on Removal percentage of MB dye by Cd/ZnO nanoparticles on photocatalytic degradation MB dye.

process depend on the adsorption process as the initial step, therefore the surface will attach to the MB dye as in suggested figure as show (Fig. 5). This increase can be attributed to a more significant

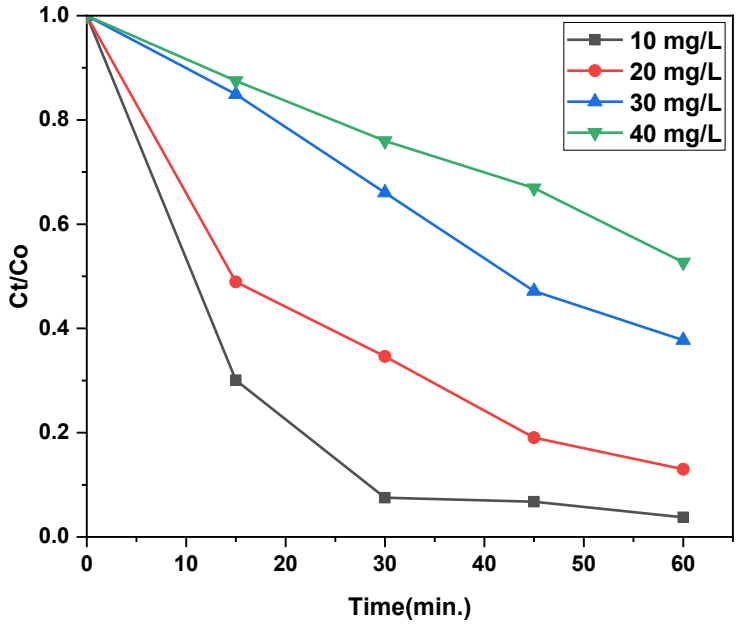

Fig. 8. Photocatalytic degradation at different concentration of MB dye onto Cd/ZnO nanoparticles.

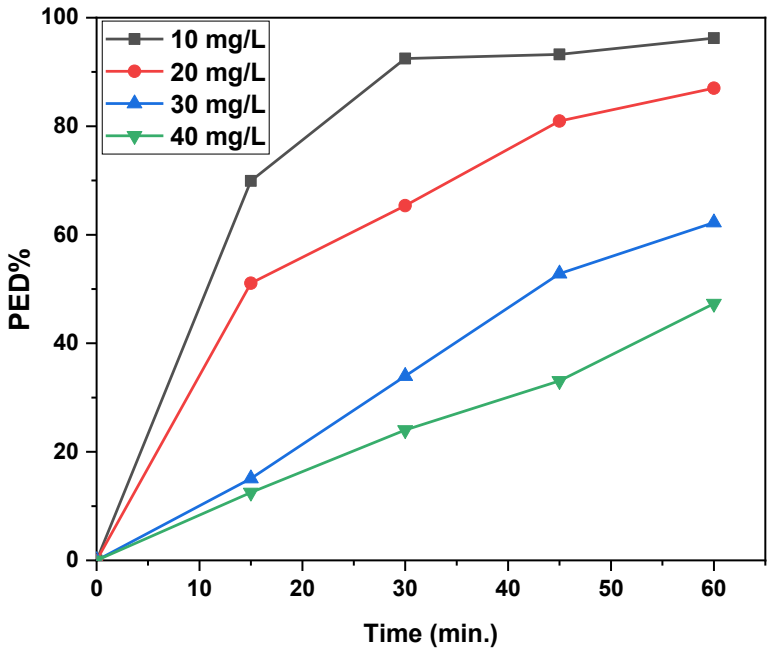

Fig. 9. Removal percent MB dye at different initial concentration.

number of active sites available for the reaction, as illustrated in Fig. 6. The results indicate that the degradation rate of the modified catalyst increased with the photocatalyst concentration from 0.1 to 0.4 g/L. However, the available active sites for dye adsorption on the catalyst surface reach a limit at a concentration of 0.3 g/L. Beyond this concentration, the degradation rate began to decrease. At higher concentrations, the intermediates formed during the reactions occupied the vacant sites, which hindered further substrate degradation. Consequently, the percentage of decomposition either decreased or remained constant[25, 26]. This outcome is reflected in the percentage of optical efficiency (E%) relative to the catalyst concentration, as shown in Fig. 7.

Effect of concentration of MB dye

The impact of initial concentration (ranging from 10 to 40 mg/L) on the photocatalytic degradation of MB dye was investigated using a catalyst concentration of 0.2 g/L, a light intensity of 1.27 mW/cm², and a temperature of 25 °C. The results, shown in Fig. 8, indicate that the rate of photocatalytic degradation decreased gradually as the initial concentration of the MB dye increased. This trend can be attributed to the observation that a concentration of 20 mg/L was optimal, as it provided the largest surface area for Cd/ZnO nanoparticles. At this concentration, the nanoparticles can absorb the maximum number of excitation photons, resulting in a higher concentration of activated Cd/ZnO nanoparticles. As the dye concentration increased, the solution became more intensely colored, which obstructed the penetration of radiation to the catalyst surface. Consequently, the ratio of free radicals (·OH) to dye molecules decreased, resulting in reduced photodegradation efficiency. However, an MB dye concentration of 20 mg/L yielded the highest photocatalytic degradation efficiency of 100% [27, 28]. The relationship between the percentage of photocatalytic degradation efficiency and the concentration of MB dye is illustrated in Fig. 9.

CONCLUSION

A cadmium sulfide-zinc oxide nanoparticle photocatalyst was successfully synthesized at a low temperature using a simple, environmentally friendly, and easily controllable catalyst-free hydrothermal technique. The synthesized cadmium sulfide photocatalyst exhibited a three-dimensional structure with high crystallinity and excellent optical properties. This catalyst was employed for the decomposition of the cationic azo dye methylene blue.1. The prepared CdS/ZnO nanoparticles show vigorous photocatalytic activity for dye removal. Among the samples tested, CdS-doped ZnO demonstrated the highest photocatalytic performance. The rate of photodegradation increased with higher light intensity. In contrast, as the concentration of pollutants increased, the rate of photodegradation decreased. The photocatalytic CdS/ZnO can be reused effectively. A concentration of 20 mg/L yielded the highest photocatalytic degradation efficiency of 90%. The results indicate that the degradation rate of the modified catalyst increased with the photocatalyst concentration from 0.1 to 0.4 g/L. However, the available active sites for dye adsorption on the catalyst surface reach a limit at a concentration of 0.3 g/L.

CONFLICT OF INTEREST

The authors declare that there is no conflict of interests regarding the publication of this manuscript.

REFERENCES

1. Gao M, Ma Y, Qi L, Liang J, Si Y, Zhang Q. Anatase TiO_2 nanocrystals via dihydroxy bis (ammonium lactato) titanium (IV) acidic hydrolysis and its performance in dye-sensitized solar cells. J Porous Mater. 2018;25(5):1499-1504.
2. Pino E, Calderón C, Herrera F, Cifuentes G, Arteaga G. Photocatalytic Degradation of Aqueous Rhodamine 6G Using Supported TiO_2 Catalysts. A Model for the Removal of Organic Contaminants From Aqueous Samples. Frontiers in chemistry. 2020;8:365-365.
3. Shichi T, Takagi K. Clay minerals as photochemical reaction fields. Journal of Photochemistry and Photobiology C: Photochemistry Reviews. 2000;1(2):113-130.
4. Fox MA, Dulay MT. Heterogeneous photocatalysis. Chem Rev. 1993;93(1):341-357.
5. Is it Photocatalytic Degradation of Textile Dyes a Friendly Method? Methyl Violet Dye as a Model for Application in Aqueous Solutions in the Presence of Commercial TiO_2. International Journal of Recent Technology and Engineering. 2019;8(2S3):1455-1457.
6. Mahdi ZS, Aljeboree AM, Rasen FA, Salman NAA, Alkaim AF. Synthesis, Characterization, and Regeneration of Ag/TiO_2 Nanoparticles: Photocatalytic Removal of Mixed Dye Pollutants. RAiSE-2023; 2024/01/26: MDPI; 2024. p. 216.
7. Al-Obaidy SSM, Greenway GM, Paunov VN. Enhanced Antimicrobial Action of Chlorhexidine Loaded in Shellac Nanoparticles with Cationic Surface Functionality. Pharmaceutics. 2021;13(9):1389.
8. Xiao H, Shan Y, Zhang W, Huang L, Chen L, Ni Y, et al. C-nanocoated ZnO by TEMPO-oxidized cellulose templating

for improved photocatalytic performance. Carbohydr Polym. 2020;235:115958.
9. Poyatos JM, Muñio MM, Almecija MC, Torres JC, Hontoria E, Osorio F. Advanced Oxidation Processes for Wastewater Treatment: State of the Art. Water, Air, and Soil Pollution. 2009;205(1-4):187-204.
10. Aljeboree AM, Alkaim AF. Removal of Antibiotic Tetracycline (TCs) from aqueous solutions by using Titanium dioxide (TiO_2) nanoparticles as an alternative material. Journal of Physics: Conference Series. 2019;1294(5):052059.
11. Jin Z, Gao L, Zhou Q, Wang J. High-performance flexible ultraviolet photoconductors based on solution-processed ultrathin ZnO/Au nanoparticle composite films. Sci Rep. 2014;4:4268-4268.
12. Khodabakhshi A, Mohammadi-Moghadam F, Amin MM, Hamati S, Hayarian S. Comparison of Paraquat Herbicide Removal from Aqueous Solutions using Nanoscale Zero-Valent Iron-Pumice/Diatomite Composites. International Journal of Chemical Engineering. 2021;2021:1-12.
13. Algubury HY. Study The Activity Of Titanium Dioxide Nanoparticle Using Orange G Dye. Malaysian Journal of Science. 2016;35(2):340-353.
14. Mirzaei A, Chen Z, Haghighat F, Yerushalmi L. Removal of pharmaceuticals from water by homo/heterogonous Fenton-type processes – A review. Chemosphere. 2017;174:665-688.
15. Fabryanty R, Valencia C, Soetaredjo FE, Putro JN, Santoso SP, Kurniawan A, et al. Removal of crystal violet dye by adsorption using bentonite – alginate composite. Journal of Environmental Chemical Engineering. 2017;5(6):5677-5687.
16. Adsorption of Textile Dyes In the Presence Either Clay or Activated Carbon as a Technological Models: A Review. Journal of critical reviews. 2020;7(05).
17. Demirbas A. Agricultural based activated carbons for the removal of dyes from aqueous solutions: A review. J Hazard Mater. 2009;167(1-3):1-9.
18. Ashley A, Thrope B, Choudhury MR, Pinto AH. Emerging investigator series: photocatalytic membrane reactors: fundamentals and advances in preparation and application in wastewater treatment. Environmental Science: Water Research and Technology. 2022;8(1):22-46.
19. Saravanan R, Gupta VK, Prakash T, Narayanan V, Stephen A. Synthesis, characterization and photocatalytic activity of novel Hg doped ZnO nanorods prepared by thermal decomposition method. J Mol Liq. 2013;178:88-93.
20. Tsega M, Dejene FB. Morphological, thermal and optical properties of TiO_2 nanoparticles: The effect of titania precursor. Materials Research Express. 2019;6(6):065041.
21. Van Viet P, Trung NC, Nhut PM, Van Hieu L, Thi CM. The fabrication of the antibacterial paste based on TiO_2 nanotubes and Ag nanoparticles-loaded TiO_2 nanotubes powders. J Exp Nanosci. 2017;12(1):220-231.
22. Maryudi M, Amelia S, Salamah S. Removal of Methylene Blue of Textile Industry Waste with Activated Carbon using Adsorption Method. Reaktor. 2019;19(4):168-171.
23. Zhang Y, Fu F, Li Y, Zhang D, Chen Y. One-Step Synthesis of Ag@TiO_2 Nanoparticles for Enhanced Photocatalytic Performance. Nanomaterials (Basel, Switzerland). 2018;8(12):1032.
24. Zhang J, Cha JK, Fu G, Cho EJ, Kim HS, Kim SH. Aerosol processing of Ag/TiO_2 composite nanoparticles for enhanced photocatalytic water treatment under UV and visible light irradiation. Ceram Int. 2022;48(7):9434-9441.
25. Burek BO, Bahnemann DW, Bloh JZ. Modeling and Optimization of the Photocatalytic Reduction of Molecular Oxygen to Hydrogen Peroxide over Titanium Dioxide. ACS Catalysis. 2018;9(1):25-37.
26. Song J, Sun G, Yu J, Si Y, Ding B. Construction of ternary Ag@ZnO/TiO_2 fibrous membranes with hierarchical nanostructures and mechanical flexibility for water purification. Ceram Int. 2020;46(1):468-475.
27. Saeed M, Muneer M, Khosa MKK, Akram N, Khalid S, Adeel M, et al. Azadirachta indica leaves extract assisted green synthesis of Ag-TiO_2 for degradation of Methylene blue and Rhodamine B dyes in aqueous medium. Green Processing and Synthesis. 2019;8(1):659-666.
28. Kaur J, Singhal S. Heterogeneous photocatalytic degradation of rose bengal: Effect of operational parameters. Physica B: Condensed Matter. 2014;450:49-53.